

Winner of the 2015 EACTS Hans G. Borst Award

Cite this article as: Numata S, Itatani K, Kanda K, Doi K, Yamazaki S, Morimoto K *et al.* Blood flow analysis of the aortic arch using computational fluid dynamics. *Eur J Cardiothorac Surg* 2016;49:1578–85.

Blood flow analysis of the aortic arch using computational fluid dynamics[†]

Satoshi Numata*, Keiichi Itatani, Keiichi Kanda, Kiyoshi Doi, Sachiko Yamazaki, Kazuki Morimoto, Kaichiro Manabe, Koki Ikemoto and Hitoshi Yaku

Department of Cardiovascular Surgery, Kyoto Prefectural University of Medicine, Kyoto, Japan

* Corresponding author. Department of Cardiovascular Surgery, Kyoto Prefectural University of Medicine, 465 Kajicho Kamigyo, Kyoto 6020841, Japan. Tel: +81-75-2515752; fax: +81-75-2515752; e-mail: snumat@yahoo.co.jp (S. Numata).

Received 14 September 2015; received in revised form 17 November 2015; accepted 19 November 2015

Abstract

OBJECTIVES: To obtain predictive information regarding aortic disease, we evaluated how blood flow inside the aortic arch was influenced by thoracic aortic aneurysms. In addition, to reveal the optimal intraoperative management in these cases, we examined blood flow during right subclavian arterial (rSCA) perfusion using computational fluid dynamics (CFD).

METHODS: Patient-specific models of the aortic arch were made with six different patterns based on the computed tomographic images. CFD models with finite volume methods were created to simulate the physiological pulsatile flow including the peripheral reflection wave, characteristic impedance and autonomous regulation system. Flow stream patterns, wall shear stress (WSS) and the oscillatory shear index (OSI) were calculated during one cardiac cycle. Furthermore, flow streamlines during rSCA perfusion were simulated under different perfusion flows.

RESULTS: Aortic dilatation caused vortical disturbed flow in a dilated space, resulting in turbulent flow not only inside the aneurysm but also in the proximal and/or distal normal aortic portion. In patients with a dilated thoracic aorta, there was a helical spiral flow with a circumferential vortex in systole. In patients with an arch aneurysm, turbulent flow inside the aneurysm caused a high OSI at the tip of the aneurysm. A high OSI was detected at the orifice of the supra-aortic branches, sinotubular junction, posterior lateral side of the ascending aorta and lesser curvature of the proximal descending aorta. rSCA perfusion revealed that the right common carotid artery was perfused by blood flow from rSCA throughout the cardiac cycle. With 75% of the flow from the rSCA, blood flow from the heart reached the left common carotid and subclavian artery only during a short period during the peak of systole.

CONCLUSIONS: A dilated aorta causes a turbulent flow pattern in the aortic arch. The high OSI site was similar to the favourite entry site for acute aortic dissection, indicating the causal relationship between mechanical stress and acute aortic dissection. rSCA cannulation might be cerebroprotective from ascending aortic plaque.

Keywords: Aortic dissection • Wall shear stress • Oscillatory shear index • Aneurysm • Fluid dynamics

INTRODUCTION

Currently, surgical strategies for aortic diseases are decided mainly based on symptoms or morphological factors, such as the maximal diameter, saccular shape and false lumen presence [1]. Although size of the aorta is an effective predictor, progress is needed to achieve better prediction from other parameters. It is obvious that haemodynamic parameters, such as blood flow velocity, blood

pressure and wall shear stress (WSS), are closely related with the pathophysiology of aortic diseases. These fluid dynamic parameters should also be considered when the surgical strategy is discussed. Computational fluid dynamics (CFD) has been introduced to clinical practice recently [2, 3], and it enables the examination of detailed flow dynamics, including WSS and total pressure, using a 3D model based on patient-specific computed tomography data. It also enables the visualization of detailed haemodynamics in a virtual situation, such as intraoperative and/or postoperative cardiovascular surgical states.

[†]Presented at the 29th Annual Meeting of the European Association for Cardio-Thoracic Surgery, Amsterdam, Netherlands, 3–7 October 2015.

In this study, we evaluated blood flow from the aortic root to the proximal descending aorta using CFD. In Study 1, we selected 5 patients with a dilated thoracic aorta and 1 patient with a normal-sized thoracic aorta; the relationship between haemodynamic parameters and the likely site for aortic pathology, such as acute aortic dissection, was evaluated. In Study 2, we simulated the right subclavian artery (rSCA) cannulation as the inflow of the cardiopulmonary bypass and analysed the blood flow inside the aortic arch.

MATERIALS AND METHODS

Patient profiles

Patient 1 is a 41-year old gentleman with Marfan syndrome who was diagnosed with a typical pear-shaped annuloaortic ectasia (AAE) with moderately severe aortic valve regurgitation and a ventricular septal defect. He underwent valve-sparing aortic root replacement (remodelling procedure) and ventricular septal defect repair. Patient 2 was also diagnosed with AAE with moderately severe aortic valve regurgitation. This patient also had a dilated ascending aorta and a proximal aortic arch; therefore, he underwent remodelling procedure and ascending aorta replacement using deep hypothermic circulatory arrest. Patient 3 had severe aortic valve stenosis with a unicuspid aortic valve. The maximum diameter of the mid-ascending aorta was 45 mm; therefore, he underwent aortic valve replacement with a tissue valve and ascending aorta replacement. Patient 4 is an 80-year old gentleman who was diagnosed with a distal arch aneurysm from a chest X-ray. This patient underwent total arch replacement using antegrade selective cerebral perfusion and moderate hypothermic circulatory arrest using a four-branched prosthetic graft. Patient 5 was originally scheduled for an abdominal aortic aneurysm repair. Chest computed tomography for preoperative assessment showed a common trunk of the brachiocephalic artery and right common carotid artery, a so-called bovine arch. The distal aortic arch was slightly dilated to 33 mm. We used this computed tomography data for the study. An abdominal aortic aneurysm repair was performed successfully. However, 3 years after the repair, the patient presented with complicated acute type A dissection, which required an emergency total arch replacement. From the intraoperative findings, there was an intimal tear at the anterior side of the ascending aorta. Patient 6 underwent coronary artery bypass grafting for stable angina. Postoperatively, the bypass graft was evaluated with computed tomography; the size of the thoracic aorta was normal. Computed tomographic images were used for control images for this study.

Study design

Study 1. We analysed 5 patients with an ascending aortic and/or aortic arch pathology as well as one normal-sized thoracic aorta patient. Pulsatile cardiac flow from one cardiac cycle was simulated, and a 3D movie was made to evaluate flow velocity, WSS and oscillatory shear index (OSI).

Study 2. We evaluated right subclavian artery (rSCA) perfusion using CFD in Patient 2. For simulating the rSCA cannulation, Patient 2's computed tomography data were modified by 3D-coat, a 3D computer graphics software program (PIGWAY®, Ukraine), which

mimicked the end-to-side anastomosis between the rSCA and an 8-mm prosthetic graft. Perfusion flow through the rSCA was set to 2.50 l/min (50% flow) and 3.75 l/min (75% flow) at a constant steady flow. Additionally, a 3D movie was made of one cardiac cycle to evaluate the streamline of the blood flow, velocity, WSS and OSI.

COMPUTATIONAL SIMULATION METHODS

Geometries and meshes

The details of our computational analysis methods have been previously described [2-4] and shown in Fig. 1. Data for analyses were acquired by thin slice, early phase enhanced multidetector-row computed tomography. Image data in a Digital Imaging and Communications in Medicine format were transferred into 3D patient-specific geometries using the medical open source imaging software Osirix (Osirix Foundation). Computational meshes were created with the commercial software ANSYS-ICEM CFD 15.0 or 16.0 (ANSYS® Japan, Tokyo, Japan). More than 2 000 000 cells with tetrahedral meshes and 3 boundary-fitted prism layers were generated. The mesh numbers were defined from our previous mesh refinement study [4], and the prism layers were generated at the boundaries to accurately measure WSS near the wall regions.

Boundary conditions

To imitate the flow around the valve leaflets, inlet boundaries for the ascending aorta were extruded to five times their diameters to develop the velocity profiles. The inlet boundary conditions in the ascending aorta were set as the mass flow boundary conditions with a pulsatile wave, and those in the subclavian perfusion cannula were set as the constant steady flow rate conditions. Cardiac outputs were set at 5.0 l/min. The outlet boundaries for the supra-aortic branches, descending aorta and bilateral coronary arteries were extended to 50 times the diameter of each vessel to obtain a stable flow split to the branches based on our previous validation study with aortic CFD modelling [4]. The outlet boundary conditions were given as the pressure boundary conditions, which reflected the external forces from outside the analysis domain. One of the main external forces from the peripheral tissue is a reflection wave; thus, to realize the reflection, the following formula was used:

$$P_{\text{measured}} - Z_0 Q_{\text{inlet}} \quad (1)$$

where P_{measured} was the measured pressure wave and Q_{inlet} was the total inlet flow. Z_0 was the characteristic impedance of the aorta. To realize the inertial properties of the vessel wall, we set the inertial term with inductance L to maintain the intravessel pressure with the flow change and added it into [1]:

$$-L \frac{dQ_{\text{inlet}}}{dt} \quad (2)$$

In addition, aortic flow is typically regulated by the autonomous system, such as the vasovagal reflex, to prevent flow voids from the neck vessels or excessive current to the lower half body, which could occur when the flow decreased in the late systolic phase.

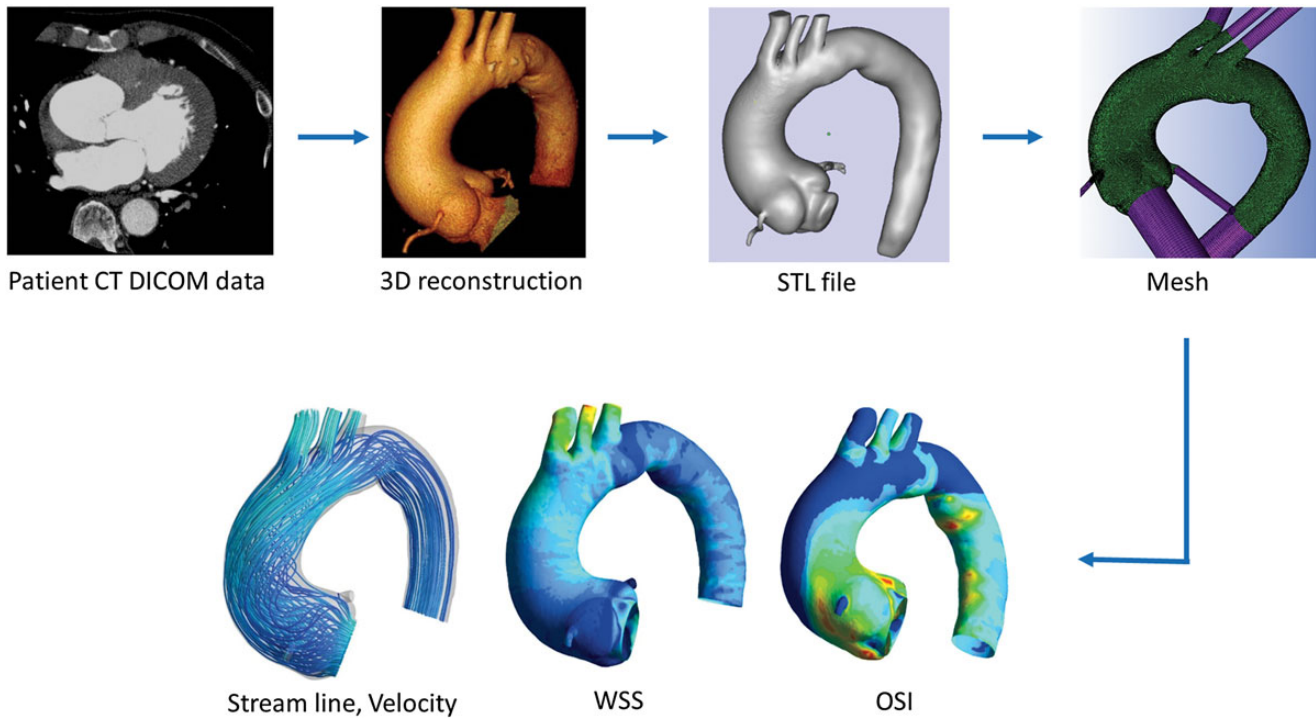


Figure 1: Work progress of analysis using computational fluid dynamics. CT: computed tomography; DICOM: digital Imaging and communications in medicine; OSI: Oscillatory shear index; STL: stereo lithography; WSS: wall shear stress.

To imitate vascular bed constriction or dilatation according to the abnormal flow split, we added the autonomous regulation term as

$$R_{\text{peripheral}} \times H(Q_{\text{descending}} - Q_{\text{inlet}}) \quad (3)$$

where $R_{\text{peripheral}}$ was the peripheral arterial resistance (constant) and $H(x)$ was the Heaviside function.

Outlet boundaries in the coronary arteries were set as mass flow boundary conditions with pulsatility, and 2.5% of the total aortic flow was given in the right and left coronary arteries. The vessel walls, including the extended boundary walls, were assumed to be rigid (Fig. 2).

Turbulent pulsatile flow simulations

The finite volume solver package ANSYS-FLUENT 15.0 or 16.0 (ANSYS®, Inc.) was used to solve the Navier–Stokes equation of incompressible transient Newtonian fluid. The blood properties were set as follows: 1060 kg/m³ for density and 0.004 kg/m/s for viscosity. Because the Reynolds number was approximately 4000 in the peak systolic phase, we analysed the turbulent flow simulation using RNG k-ε models. In the transient flow simulation, each time step was set to 10⁻⁵ s to reduce the Courant number to the sufficient level. The convergence criteria were set to 10⁻⁵ times the residual for all of the degrees of the parameters at each time step.

Wall shear stress and oscillatory shear index

From the calculated results, we evaluated WSS and OSI. Because WSS is a vector with force and direction, its fluctuation in one cardiac cycle is also important information. OSI was defined as

follows:

$$\text{OSI} = \frac{1}{2} \left(1 - \frac{|\int_0^T \overrightarrow{\text{WSS}} dt|}{\int_0^T |\overrightarrow{\text{WSS}}| dt} \right) \quad (4)$$

RESULTS

Study 1

An aneurysm causes vortical disturbed flow in a dilated space, resulting in turbulent flow not only inside the aneurysm but also in the proximal and/or distal normal aortic portion (Fig. 3, Video 1). In Patients 1, 2 and 3 with dilated aortic roots or ascending aortas, there was a helical spiral flow with a circumferential vortex during early systole in the ascending aorta. In peak systole, the streamline from the ascending aorta to the aortic arch remained helical. In Patients 4, 5 and 6 without ascending aortic dilatation, the streamline in peak systole was almost laminar from the ascending to descending aorta. In Patients 4 and 5, there was a vortical flow inside the distal arch aneurysm in systole, and the turbulent flow inside the arch aneurysm caused disturbed reflection wave, resulting in turbulence in the ascending aorta. In all patients, including the control case, the vortex flow at the lesser curvature of the proximal descending aorta was observed in late systole. These particular flow changes caused a characteristic distribution of WSS and OSI in each patient (Fig. 3, Videos 1 and 2).

In all patients, except Patient 2, who did not have an obvious constriction of the sinotubular junction, WSS in peak systole was high in the sinotubular junction and the lesser curvature of the descending aorta.

A high OSI was detected at the orifice of the supra-aortic branches, sinus of Valsalva, and lesser curvature side of the

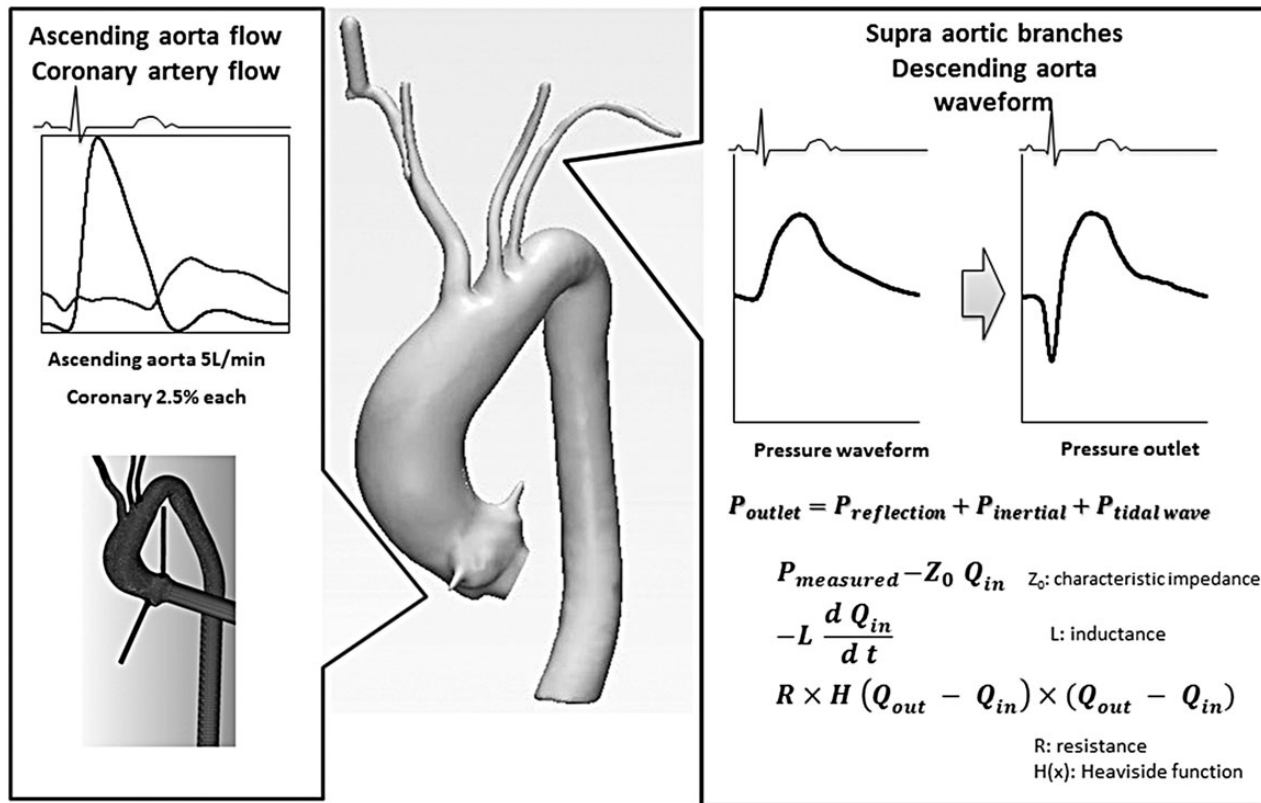


Figure 2: Definition of inlet and outlet boundary condition.

proximal descending aorta in all patients (Fig. 3). From the posterior-lateral side of the aortic root to the arch, there was a high OSI 'strap' to a varying degree in all patients. In patients with a distal arch aneurysm (Patients 4 and 5), there was a high OSI area at the most dilated part of aneurysmal wall.

Study 2

In this study, 75 and 50% of the total flow were simulated. In both simulations, blood flow from the rSCA cannulation perfused the right common carotid artery throughout the entire cardiac cycle. With the 75% flow simulation, the left common carotid artery and the left subclavian artery were perfused by blood flow from the rSCA during almost all of the cardiac cycle, except during the peak systolic phase. With 50% flow, during systole, the left common carotid artery and the left subclavian artery were perfused by both rSCA cannulation and the heart itself (Fig. 4, Video 2).

DISCUSSION

Acute aortic dissection is often a surgical emergency. The surgical results of Type A aortic dissection repair are still ~10% in our country though the number of surgical cases is increasing [5]. There are many controversial issues associated with aortic dissection that surgeons have to overcome. In most cases, aortic dissection is associated with a history of hypertension or connective tissue diseases, such as Marfan syndrome. In a

connective tissue disease patient, cystic medial necrosis plays an important role in the pathogenesis of aortic dissection [6]. In patients with a history of hypertension, it has been reported that there is a significant loss of inter-laminar elastin in the media and destruction of the elastic lamina, which could result in the weakness of the media against various forces [7–9]. The common finding in the settings of both Marfan syndrome and hypertension is that a weakened area exists in the media. It could be hypothesized that, prior to the onset of aortic dissection, medial degeneration progresses first and in this circumstance, bleeding from the vasa vasorum or an intimal tear triggers acute aortic dissection [10]. We believe that WSS also may play an important role in medial degeneration. It is well recognized that a higher or lower WSS may cause intimal dysfunction, which could result in the progression of atherosclerosis [11, 12]. Furthermore, because of the non-slip boundary mechanical equilibrium of forces, WSS, which is a mechanical force generated by the blood flow to shear the endothelial layer of the vessel wall, will separate the inner and outer layers of the aorta. This shear force could stress the medial tissue and result in degeneration. OSI has been reported as an important haemodynamic parameter that is highly associated with the progression of atherosclerosis by inducing radical oxygen production of the endothelial cells [13, 14]. OSI describes the degree of deviation of the WSS from its mean direction. Therefore, OSI may be more closely associated with the degeneration of the media in comparison with WSS.

In this study, we evaluated the WSS, flow velocity and OSI of the aortic arch in patients with an aortic arch pathology, such as an ascending aorta aneurysm, and/or an AAE. We used CFD to calculate the haemodynamic parameters and made a 3D movie of the

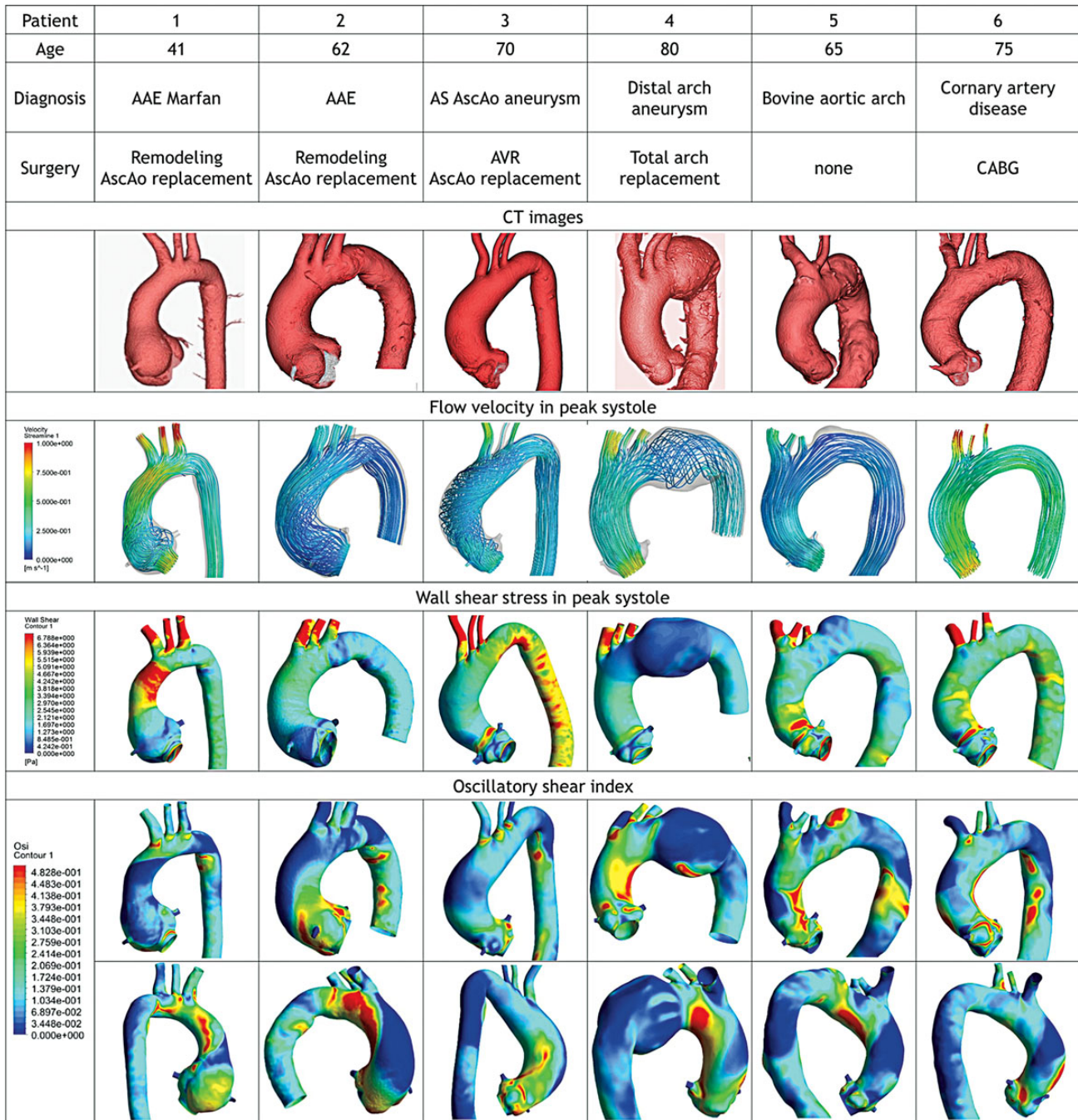
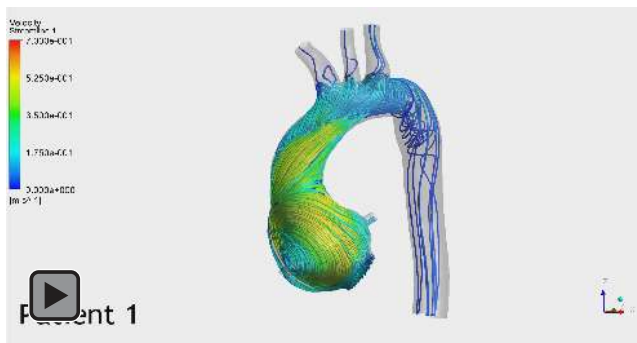


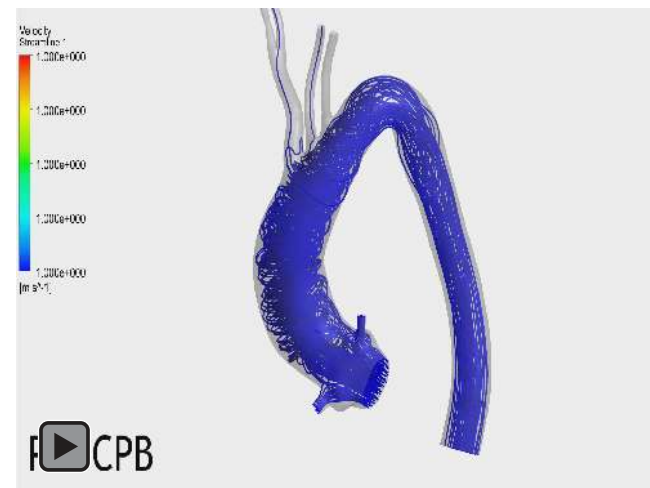
Figure 3: Results of computational fluid dynamics analysis. AAE: annuloaortic ectasia; AS: aortic valve stenosis; AscAo: ascending aorta; CABG: coronary artery bypass grafting; CT: computed tomography.

pulsatile flow. Furthermore, the localization of the WSS, flow velocity and OSI of the aortic arch was estimated and compared with the likely site for aortic dissection. According to the autopsy studies [15, 16], an intimal tear is usually transverse and involves more than half of the circumference. The likely site for an intimal tear is located 1–3 cm distal to the coronary artery orifice and the descending aorta just distal to the left subclavian artery. From our study results, a high OSI area is located around the sinotubular junction, near the bifurcation of the neck vessels and the lesser curvature side of the proximal descending aorta in all studied

cases. These areas are close to the likely site of aortic dissection. This might suggest the relationship between a high OSI and medial degeneration that could initiate acute aortic dissection. Patient 5 presented with a complicated acute type A aortic dissection 3 years after the examination of the computed tomography that we used for this computational fluid analysis. The patient successfully underwent emergency total arch replacement; intraoperative findings showed that an intimal tear was present on the anterior side of the ascending aorta. From our study, OSI was high in Patient 5 in the area where the tear was found during surgery.



Video 1: Four-dimensional evaluation of flow streamline and wall shear stress.



Video 2: Four-dimensional evaluation of right axillary artery cannulation simulation.

This finding may support the hypothesis of a relationship between OSI and medical degeneration.

In Patients 4 and 5, who had distal arch aneurysms, there was a high OSI area at the localized part of the aortic aneurysm. These areas might progress intimal dysfunction and atherosclerotic changes more rapidly than in the other part of the aorta. These findings suggest a risk of rupturing the aortic aneurysm.

In Study 2, we evaluated the aortic arch blood flow when the rSCA was used as the inflow of the cardiopulmonary bypass. The rSCA is a popular cannulation site, particularly for acute aortic dissection or an aortic arch aneurysm, and a lower incidence of stroke with the right subclavian or axillary artery cannulation has been reported [17–19]. Even with conventional coronary surgery or valve surgery, rSCA cannulation could be considered to avoid potential embolization by an atheromatous plaque in the ascending aorta [20]. Hedayati *et al.* compared right axillary artery cannulation with ascending aorta cannulation by evaluating a microsphere distribution of distal organs in dogs. Their findings showed significantly fewer microspheres in the brain with right axillary artery cannulation. They concluded that axillary artery cannulation is cerebroprotective because an altered blood flow pattern during axillary artery cannulation may produce retrograde brachiocephalic artery blood flow and deflect emboli from the ascending aorta and arch towards the descending aorta [21]. Another experimental study [22] tried to show the risk and benefit of subclavian artery cannulation; however, there is no study that has visualized the blood flow inside the aortic arch with rSCA cannulation. In this study, we evaluated

the blood flow of the aorta and supra-aortic vessels through rSCA perfusion by CFD. With both 50 and 75% flow simulations, the blood streamline from the rSCA produced retrograde flow of the brachiocephalic artery and antegrade flow of the supra-aortic branches. Retrograde flow from the brachiocephalic artery deflects blood flow from the heart itself. This may explain how the atherosclerotic emboli were protected by the rSCA perfusion especially when the atherosclerotic plaque was located on the ascending aorta or proximal aortic arch.

Study limitation

With CFD, it is controversial whether calculated results, such as the flow velocity, WSS and OSI, are as accurate as the haemodynamic parameters that are directly measured by a catheter or echocardiography. We have established CFD models referring to the results of 4D magnetic resonance imaging [23]. However, controversial issues for making an accurate CFD model remain. Firstly, to reduce the calculation cost, we applied a fixed boundary condition in the present study, but wall motion with elastic properties should be included to increase the accuracy. However, estimation of the elastic vessel property distribution in atherosclerotic aortic disease is quite difficult; thus, a simple fluid–structure interaction calculation cannot solve the problem. Secondly, validation regarding the flow split to each branch, or flow streamlines, was insufficient. Even MRI flow measurements have limitations in spatial and temporal resolution; thus, there are technical limitations regarding the validation of CFD modelling. Thirdly, a limited number of cases were analysed in the present study. Although the typical patterns of thoracic aortic aneurysms were included in these 6 cases, further accumulation of CFD calculation cases would reveal the prognostic and diagnostic clinical meanings of the WSS and its related parameters. Fourthly, because the present study analyses clinical cases, pathological changes in the endothelial tissue cannot be examined in all portions of the aortic arch. The accumulated analysis results and validation and verification with *in vivo* measurements and clinical outcomes warrant further studies. Fifthly, one of the biggest limitations of present study is not including the vessel wall motion. Future studies should be performed based on the fluid–structure interaction modelling, considering accurate elastic property and surrounding tissues from patient-specific images [24], and based on the accurate boundary layer turbulence flow simulation and on the accurate OSI calculation that truly makes impact on the endothelium functions and intimal damage [25]. Finally, idealized boundary conditions were applied in this study for comparing impact of each aortic arch pathology. Patient's specific cardiac function, aortic valve pathology and hypertension were not considered for our calculations. Therefore, there might be a discrepancy between individual measured data and calculated data by our study.

CONCLUSION

In conclusion, with CFD, we could evaluate the haemodynamic parameters as 3D images during one cardiac cycle. Inside a dilated aorta, there was a vortex flow that resulted in turbulent flow at the proximal and distal part of the dilated aorta. These changes caused a characteristic distribution of WSS and OSI in each patient. The location of the OSI might be related with the

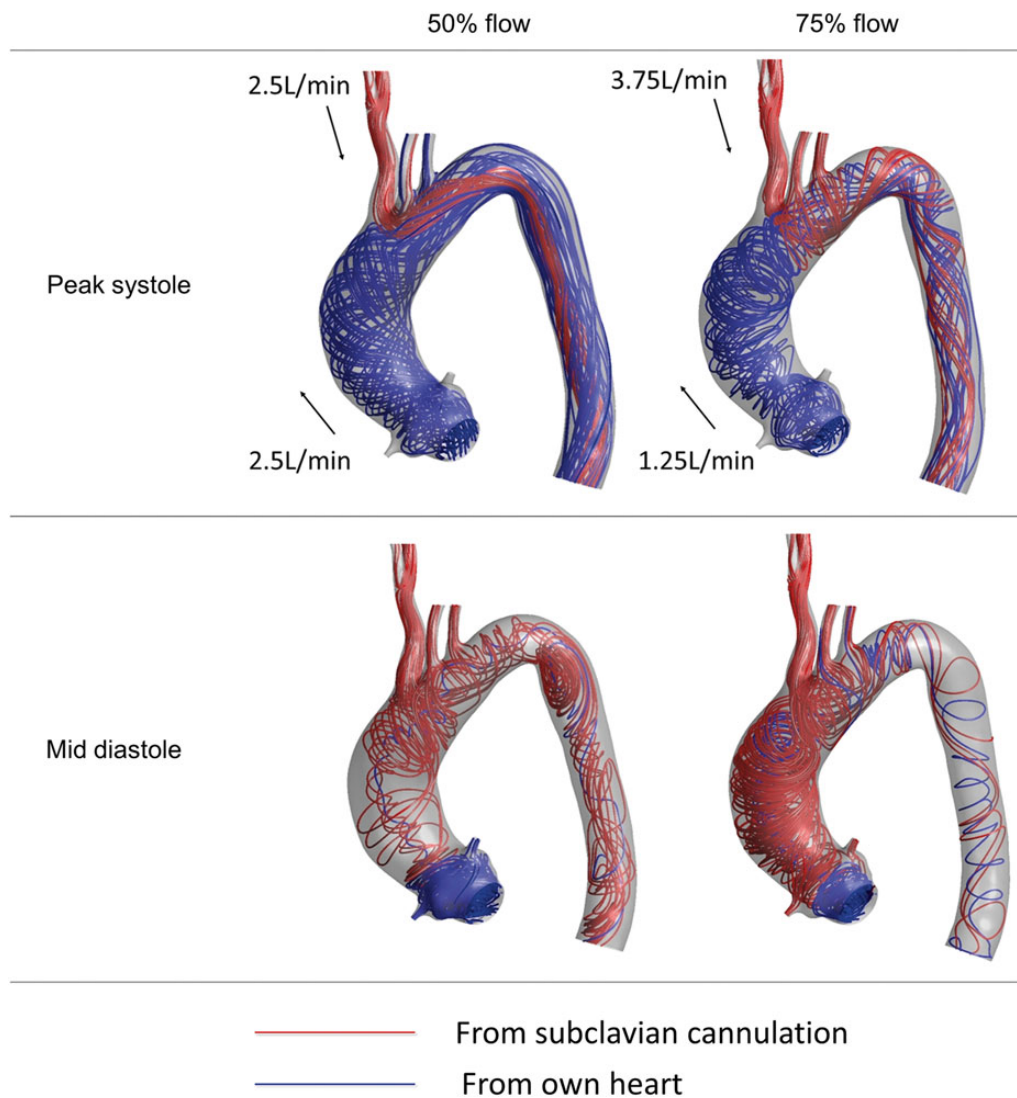


Figure 4: Results of right subclavian artery cannulation simulation.

likely site of acute aortic dissection entry and aneurysmal changes of the aorta.

Conflict of interest: none declared.

REFERENCES

- [1] Erbel R, Aboyans V, Boileau C, Bossone E, Di Bartolomeo R, Eggebrecht H *et al.* 2014 ESC guidelines on the diagnosis and treatment of aortic diseases. *Eur Heart J* 2014;35:2873–926.
- [2] Itatani K, Miyaji K, Qian Y, Liu JL, Miyakoshi T, Murakami A *et al.* Influence of surgical arch reconstruction methods on single ventricle workload in the Norwood procedure. *J Thorac Cardiovasc Surg* 2011;144:130–8.
- [3] Koyama S, Itatani K, Yamamoto T, Miyazaki S, Kitamura T, Taketani T *et al.* Optimal bypass graft design for left anterior descending and diagonal territory in multivessel coronary disease. *Interact CardioVasc Thorac Surg* 2014;19:406–13.
- [4] Qian Y, Liu JL, Itatani K, Miyaji K, Umezu M. Computational hemodynamic analysis in congenital heart disease: simulation of the Norwood procedure. *Ann Biomed Eng* 2010;37:2302–13.
- [5] Okita Y. Surgery for thoracic aortic disease in Japan: evolving strategies toward the growing enemies. *Gen Thorac Cardiovasc Surg* 2015;63:185–96.
- [6] Golledge J, Eagle KA. Acute aortic dissection. *Lancet* 2008;372:55–66.
- [7] Carlson RG, Lillehei CW, Edwards JE. Cystic medial necrosis of the ascending aorta in relation to age and hypertension. *Am J Cardiol* 1970; 25:411–5.
- [8] Nakashima Y, Shiokawa Y, Sueishi K. Alterations of elastic architecture in human aortic dissecting aneurysm. *Lab Invest* 1990;62:751–60.
- [9] Kageyama N, Ro A, Tanifuji T, Kumagai T, Tatsuya M, Fukunaga T. The histopathologic study of elastic lamina and interconnecting elastic fiber in aortic media: implications for aortic dissection. *J Jpn Coll Angiol* 2005;45: 003–1009.
- [10] Angouras D, Sokolis DP, Dosios T, Kostomitsopoulos N, Boudoulas H, Skalkas G *et al.* Effect of impaired vasa vasorum flow on the structure and mechanics of the thoracic aorta: implications for the pathogenesis of aortic dissection. *Eur J Cardiothorac Surg* 2000;17:468–73.
- [11] Stone PH, Saito S, Takahashi S, Makita Y, Nakamura S, Kawasaki T *et al.* Prediction of progression of coronary artery disease and clinical outcomes using vascular profiling of endothelial shear stress and arterial wall morphology: THE PREDICTION study. *Circulation* 2012; doi:10.1161/CIRCULATIONAHA.112.096438.
- [12] Gunnungham KS, Gotlieb AI. The role of shear stress in the pathogenesis of atherosclerosis. *Lab Invest* 2005;85:9–23.
- [13] Ku DN, Giddens DP, Zarins CK, Glagov S. Pulsatile flow and atherosclerosis in the human carotid bifurcation. Positive correlation between plaque location and low and oscillating shear stress. *Atherosclerosis* 1985;5: 293–302.

- [14] Peiffer V, Sherwin SJ, Weinberg PD. Does low and oscillatory wall shear stress correlate spatially with early atherosclerosis? A systematic review. *Cardiovasc Res* 2013;99:242–50.
- [15] Nakashima Y, Kurozumi T, Sueishi K, Tanaka K. Dissecting aneurysm: a clinicopathological and histopathological study of 111 autopsied cases. *Hum Pathol* 1990;21:291–6.
- [16] Hirst AE, Varner JJ Jr, Kime W Jr. Dissecting aneurysm of the aorta: a review of 505 cases. *Medicine* 1958;37:217–79.
- [17] Numata S, Ogino H, Sasaki H, Hanafusa Y, Hirata M, Ando M *et al.* Total arch replacement using antegrade selective cerebral perfusion with right axillary artery perfusion. *Eur J Cardiothorac Surg* 2003;23:771–5.
- [18] Numata S, Tsutsumi Y, Monta O, Yamazaki S, Seo H, Sugita R *et al.* Aortic arch repair with antegrade selective cerebral perfusion using mild to moderate hypothermia of more than 28°C. *Ann Thorac Surg* 2012;91:90–6.
- [19] Ogino H, Sasaki H, Minatoya K, Matsuda H, Tanaka H, Watanuki H *et al.* Evolving arch surgery using integrated antegrade selective cerebral perfusion: impact of axillary artery perfusion. *J Thorac Cardiovasc Surg* 2008;136:641–9.
- [20] Baribeau YR, Westbrook BM, Charlesworth DC, Maloney CT. Arterial inflow via an axillary artery graft for the severely atheromatous aorta. *Ann Thorac Surg* 1998;66:33–7.
- [21] Hedayati N, Sherwood JT, Schomisch SJ, Carino JL, Markowitz AH. Axillary artery cannulation for cardiopulmonary bypass reduces cerebral micro-emboli. *J Thorac Cardiovasc Surg* 2004;128:386–90.
- [22] Minakawa M, Fukuda I, Inamura T, Yanaoka H, Fukui K, Daitoku K *et al.* Hydrodynamic evaluation of axillary artery perfusion for normal and diseased aorta. *Gen Thorac Cardiovasc Surg* 2008;56:215–21.
- [23] Itatani K. *Advance in Hemodynamic Research*. Nova Science Publishers, Inc., New York, 2015.
- [24] Bertagna L, Elia MD, Perego M, Veneziani A. Data assimilation in cardiovascular fluid–structure interaction problems: an introduction. *Fluid-Structure Interaction and Biomedical Applications, Advances in Mathematical Fluid Mechanics*. Basel: Springer 2014; doi:10.1007/978-3-0348-0822-4-6.
- [25] Takizawa K, Moorman C, Wright S, Purdue J, McPhail T, Chen PR *et al.* Patient-specific arterial fluid–structure interaction modeling of cerebral aneurysms. *Int J Numer Meth Fluids* 2011;65:308–23.

APPENDIX. CONFERENCE DISCUSSION

Scan to your mobile or go to <http://www.oxfordjournals.org/page/6153/1> to search for the presentation on the EACTS library

Dr L. Weltert (Rome, Italy): Even if we are not actually there with the technology we cannot perform STL, meshing, and then workload analysis for each and every patient as we do now with, 3D reconstruction on CT scans. I envision a future where this will be made for each patient, maybe with the EXAScale CPU coming out next year.

This kind of study helps to close the gap between basic science, or if you wish, high-hand technology and clinical practice.

Help us to further translate your study in clinical understanding. Let's comment about magnitude increase or decrease, of wall shear stress. How big is the effect and does it depend on shape or dimension or location of the aneurysm or whatever?

Also, as regarding the second part of your study, are you suggesting that we should consider more carefully an other primary target size of cannulation to obtain better perfusion, more consistently lamina perfusion flow?

Dr Numata: Regarding the first question, about wall shear stress distribution, there are many factors affecting wall shear stress from our study. Basically, what I presented this time was, the wall shear stress inside the aneurysm is pretty low. As the shape of the aortic arch becomes sharper, wall shear stress

becomes higher. The other point is that in most of the cases wall shear stress becomes higher at the ST junction.

Of course, shape of the aortic arch is very important, and as I've shown on the slide, the streamline is also very important for wall shear stress and I'm sorry, I forgot the second question.

Dr Weltert: Should we change our practice of cannulation based on your study?

Dr Numata: First of all, the reason why I tried to evaluate this simulation was, we often use the right subclavian artery cannulation for a very diseased ascending aorta patient who needs coronary artery bypass or valve replacement. Sometimes the ascending aorta is quite diseased, and we often hesitate to cannulate into the ascending aorta. So we always use the right subclavian artery cannulation for that kind of patient.

For that reason, we would like to evaluate the efficacy of the right subclavian artery using computational fluid dynamics. At the moment we are still using the right subclavian artery cannulation frequently. From this study we have confirmed the efficacy of the right subclavian artery cannulation.

Dr D. Pacini (Bologna, Italy): I'm really happy to hear this work from you because, in the clinical practice, I am doing the same. When I have a bad ascending aorta, in valve surgery as well as in coronary bypass, I prefer to put a cannula in the right axillary artery in order to reduce the risk of cerebral embolism and your data supports this approach.

Dr P. Youssefi (London, UK): I'd like to make a comment first and then ask you a couple of questions. I think computational fluid dynamics is an ever-increasing field in the importance of aortic surgery, but I think for it to be taken seriously and for the results to be analysed, it must be performed accurately and with CFD, the importance of making the simulation as patient specific as possible makes a huge impact on the results that you get.

So in the thoracic aorta, two very important factors are the boundary conditions. What inflow did you put into the aorta, and what parameters do you assign to the subclavian, the carotid arteries, and to the descending thoracic aorta? So can I ask what parameters did you set?

Dr Numata: For boundary condition for inflow, we used the flow, of 5 litres per minute.

Dr Youssefi: So that was an idealised flow?

Dr Numata: Yes, idealized. And for outflow, we used pressure. From the patient pressure waveform, for example, when we used the cardiopulmonary bypass, the patient's waveform becomes flatter. So for the right subclavian artery simulation, we use that sort of a flattened waveform as a boundary condition.

Dr P. Youssefi: We performed similar work which was presented this morning, and we found that making the inflow patient specific in a three-dimensional way made a huge impact to the results of wall shear stress and operational stress injury, seen throughout the thoracic aorta. So I just put this forward, that that is an area where we could make this even more specific because we have been making the inflow and the outflow completely patient specific.

Dr C. Etz (Leipzig, Germany): I just want to make a very brief comment. I think what you showed us in the first part of your study has the potential to be really revolutionary and change guidelines. What you need to do, you don't want to go into technical details because none of us here is really understanding the boundary condition and all these things.

What you need to do I think is to evaluate your model now with data that we have already on patients with pre- and post-aortic dissection. That would be extremely interesting. I just want to sort of recommend or encourage you to maybe get in touch with Martin Czerny and the guys from Freiburg who have a dataset on 43 patients that we have basic CAT scan data that you may be able to use your model on and evaluate, and then we don't need to keep on discussing the technical issues. Because if your model predicts what happens a couple of months later, then this is the real-time clinical evaluation that we need. And I strongly recommend to do that, and you can really save a lot of time.